sustainability

MDPI

Article

Experimental and Numerical Study on Flexural Behavior of Concrete Beams Using Notches and Repair Materials

Waseem Khan [1,*], Saleem Akhtar [1], Aruna Rawat [1] and Anindya Basu [2]

[1] Department of Civil Engineering, University Institute of Technology, Rajiv Gandhi Proudyogiki Vishwavidyalaya, Bhopal 462033, India; sargpv@gmail.com (S.A.); rawataruna14@gmail.com (A.R.)
[2] School of Pharmaceutical Sciences, Rajiv Gandhi Proudyogiki Vishwavidyalaya, Bhopal 462033, India; anindya@rgpv.ac.in
* Correspondence: wkrgpv@gmail.com

Abstract: In a concrete beam, cracking is generated on the tension side under the effect of flexure, shear, and torsional loadings. Accordingly, these weak concrete members require repair and/or strengthening to increase or restore their internal load capacity. In the current experimental and numerical investigations on concrete beams, the impact of using notches with different width to depth ratios on the ultimate flexural load under a three-point test was considered. Further, the flexural behavior performance of a notched concrete beam repaired using the three repair materials—cement mortar, bacterial mortar, and adhesive—was also examined. Consequently, a comparative study was implemented between the experimental and numerical results. A concrete damage plasticity (CDP) model was used for the finite element numerical analysis of the beams. The differences in numerical and experimental measured results ranged from 0.65 to 22.20% for the ultimate load carrying capacity. As the notch size increased, the ultimate load carrying capacity of the beam reduced. Additionally, a linear regression model was used to predict the ultimate load values at a notch width interval of 5 mm up to a maximum notch width of 100 mm. It was observed that the ultimate load capacity for a repaired beam increased as compared to the notched beam for all three repair materials under consideration. And the maximum ultimate load increased in the case of notched beams repaired using adhesive. Furthermore, in comparison to the cement mortar, the performance of the bacterial mortar in terms of the ultimate load was more. The bacterial mortar was found to be more sustainable and more durable as a repair material for concrete structures.

Keywords: bacterial mortar; concrete beam; concrete damage plasticity; flexural behavior; notch; repair materials

check for updates

Citation: Khan, W.; Akhtar, S.; Rawat, A.; Basu, A. Experimental and Numerical Study on Flexural Behavior of Concrete Beams Using Notches and Repair Materials. *Sustainability* **2024**, *16*, 2723. https://doi.org/10.3390/su16072723

Academic Editor: Constantin Chalioris

Received: 4 February 2024
Revised: 5 March 2024
Accepted: 13 March 2024
Published: 26 March 2024

Copyright: © 2024 by the authors. Licensee MDPI, Basel, Switzerland. This article is an open access article distributed under the terms and conditions of the Creative Commons Attribution (CC BY) license (https://creativecommons.org/licenses/by/4.0/).

1. Introduction

Nowadays, the sustainability of present-day civil infrastructure is being given more attention and significance. When considering the financial and environmental aspects of resource conservation into account, and the reduction in the construction industry's overall carbon footprint, repairing and/or strengthening is a more sustainable option than simply destructing and rebuilding the civil infrastructure [1]. Moreover, maintenance should be prioritized over construction. Also, in cases of historical monuments, it is not possible to demolish and replace them; thus, repairing and/or strengthening are sustainable choices to preserve them. Concrete is widely employed in the construction of the majority of civil engineering structures because of its superior shielding ability, fire rating, long service life under normal and accidental conditions, ease of construction, and relative affordability. Despite these prominent characteristics, the majority of concrete structures may become damaged when subjected to the addition of structures, overloading, accidental loads, errors in design or during the erection process, environmental conditions, etc. Consequently, these weak concrete members require repair and/or strengthening to increase or restore

their internal load capacity to resist additional external loads [2,3]. After the repair or strengthening work is successfully completed, the structural member's safety, serviceability, and durability performance can be enhanced.

A concrete beam is a horizontal member in civil engineering structures subjected to external vertical loading. Due to such loading beams, deflections occur and flexural, shear, and torsional stresses are developed. Over the past two to three decades, researchers have been endeavoring to develop numerous repair and/or strengthening techniques for concrete beams, as shown in Figure 1. When selecting any repair and/or strengthening technique, there are a number of factors to take into account, such as repair time, localized changes in the stiffness of the member, strength, ductility, cost, minimizing disturbance to occupants during repair, preserving the aesthetic appearance of structure, preserving or enhancing durability, and work safety [4,5]. Table 1 shows the various repair and strengthening materials used for concrete structures. Fiber-reinforced polymer (FRP), epoxy resin, epoxy-modified cement, and synthetic rubber emulsion are a few of the materials that have been utilized. These materials are applied in sheets, laminates, sprays, and rods.

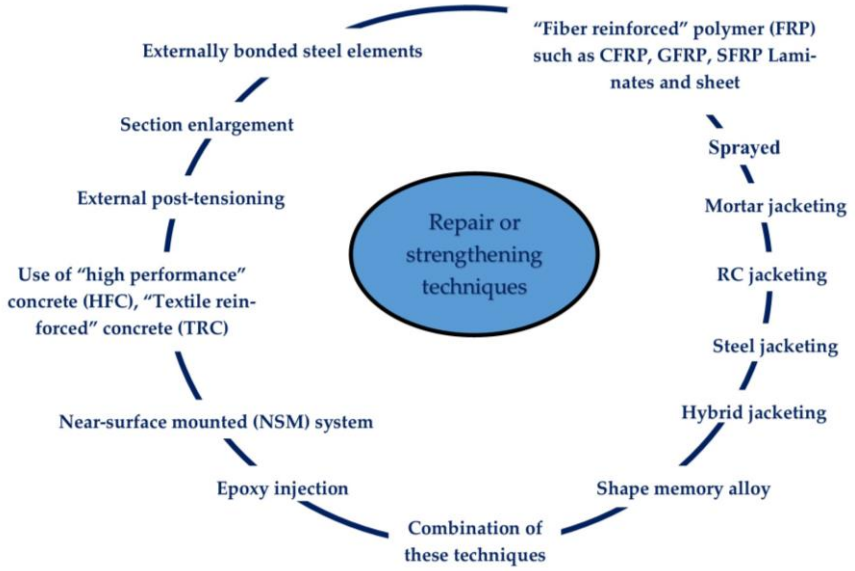

Figure 1. Various repair or strengthening techniques.

The review of previous experimental and numerical studies carried out on concrete beams are discussed herein. A numerical investigation of rectangular and T section concrete beams for bending moment capacity was carried out by [5]. An experimental investigation of prestressed concrete beams for flexural strength was performed by [6,7]; the results suggested that, in plain concrete, brittle failure occurred due to a flexural crack. In higher-strength concrete, beam brittle failure is caused by shear force and the development of a diagonal crack. The different types of openings reduce the stiffness of reinforced cement concrete (RCC) beams [8]. Dong et al. (2002) [9] suggested that the load carrying capacity and stiffness of pre-cracked RC beams can be increased by providing carbon fiber-reinforced polymer (CFRP) at the tension side of the beam; the failure of the concrete cover and the debonding between the CFRP fabric and the concrete should also be investigated. Rahim et al. (2020) investigated the experimental behavior of deep beams with web openings under a four-point load [10]. It was found that, as the size of the web opening increased, the shear strength of the concrete deep beam decreased. As discussed in Figure 1, various techniques can be used, like jacketing [11,12] and FRP [13,14].

Table 1. List of repair and strengthening materials.

Sr No.	Types of Material	Specification	Applications
		A. Concrete Repair	
1	Bonding primer	Epoxy resin	Used as bonding agent between old and new concrete structures
2	Crack repair	Low-viscosity injection resin	Moisture incentive for sealing cracks > 5 mm
3	Site batch mortars	Synthetic rubber emulsion	Used for good adhesion and water resistance
4	Smoothing mortars	Epoxy-modified cement, thixotropic, fine-textured mortar	Used for levelling and finishing of concrete, mortar, or stone surfaces
5	Structural injection material	Low-viscosity injection resin	Moisture incentive for sealing cracks > 5 mm
		B. Structural Strengthening	
1	Prefabricated CFRP plates	Pultruded carbon fiber-reinforced polymer (CFRP) laminates	Strengthening concrete, timber, masonry, steel, and fiber-reinforced polymer structures
2	FRP fabrics	Uni-directional woven carbon fiber fabric	Strengthening concrete, timber, masonry, steel, and fiber-reinforced polymer structures
3	Structural adhesives	Epoxy impregnation resin	Structural strengthening application
		C. Repairing Mortar	
1	Cementitious mortars	Polymer-modified	Repairing mortar
2	Epoxy mortar	Epoxy resin	For surface sealing and patch repair/filling mortar
3	Additives for mortars	Synthetic rubber emulsion	For waterproofing and repair

Researchers generally investigate the performance of any repair and strengthening technique, as discussed above, by imitating damages, defects and cracks in the concrete beam through embedding a notch approximately in the middle of the beam. The notch is embedded in U, V, or key-hole shapes [15,16]. The notch formation simulates the cracks or damages and then repair techniques are studied using experimental and numerical approaches. Table 2 shows the review of some of studies where the effects of notches on concrete beams were studied. Recently, carried out an experimental investigation on notched concrete beams under three-point loading for constant width and varying depths of the beam section. The results were obtained as size effect, fracture energy, failure modes, peak loads, and load–displacement analysis.

Table 2. Review of effects of notches on concrete beams.

Authors	Type of Material	Specimen Size	Loading	Properties of Material	Remarks
[17]	Polymer mortars	250 mm × 60 mm × 30 mm notches 2 mm thick at different positions, i.e., 0, 24 mm, 48 mm, and 72 mm, towards the support.	Three-point load	-	Cracked mouth-opening displacement, cracked tip-opening displacement, and values of energy release rate.

Table 2. *Cont.*

Authors	Type of Material	Specimen Size	Loading	Properties of Material	Remarks
[18]	Concrete and CFRP plate	100 mm × 100 mm × 500 mm beams with notches at the center with depths of 10 mm, 20 mm, and 30 mm, wrapped in CFRP plates with lengths of 100 mm, 200 mm, and 350 mm. Thickness of CFRP at 1 mm and adhesive at 0.5 mm.	Three-point load	f_{ck} = 41.4 MPa E_C = 32.89 GPa E_{CFRP} = 150 GPa $E_{adhesive}$ = 4.3 GPa $MI_{Concrete}$ = 8.3 × 10^6 mm^4	With and without CFRP-laminated plates, visually analysis the brittle failure, shear failures, and delaminate failure.
[19]	Foamed concrete	Foamed concrete beam 840 mm × 100 mm × 100 mm with a notch (5 mm thickness; 42 mm height) at the center.	Three-point load	$E_{Foamed\ Concrete}$ = 1000 GPa $\mu_{Foamed\ Concrete}$ = 0.2, ε = 0.2, φ = 15°	Extended finite element method (XFEM) model of foamed concrete.
[20]	Foamed concrete	Foamed concrete beam 750 mm × 150 mm × 150 mm with a 30 mm long V-notch at the center.	Cube compressive strength and three-point load test	$\rho_{concrete}$ =2400 kg/m^3, $\rho_{foamed\ concrete}$ = 1400–1600 kg/m^3	Compressive strength of cube and fracture energy of foam concrete is lower.
[21]	RCC beam, CFRP, and adhesive	RCC beam sized 3000 mm × 200 mm × 300 mm with a notch at the center of beam and 4 mm thick CFRP plates applied using a 2 mm thick layer of adhesive.	Three-point load	E_C = 30 GPa E_{CFRP} = 140 GPa $E_{Adhisieve}$ = 3 GPa μ_c = 0.18 μ_{CFRP} = 0.28 $\mu_{Adhesive}$ = 0.35	CFRP plates bond with the surface of the beam and significantly enhance the stiffness and ultimate load.
[22]	PCC beam	1640 mm × 200 mm × 400 mm in size with a notch at the center (a/d = 0.5).	Three-point load	E_C = 30,570 MPa f_{ck} = 21.9 MPa f_{tk} = 2.4 MPa	Acoustic emission (AE) and digital image correlation (DIC) techniques.
[23]	PCC beam with a steel fiber hook	A 600 mm × 150 mm × 150 mm plain concrete beam with different notch depths of 13 mm, 25 mm, and 50 mm at the center, and the a/d ratios are 0.08, 0.16 and 0.33.	Three-point load	Steel fiber of 50 mm length, 1 mm diameter, and 1130 MPa tensile strength. The water/cement ratio is 0.55, and the cement/sand/aggregate ratio is 1:2.93:2.31.	a/d ratio notch is increased by 0.08, 0.16, and 0.33 as the load carrying capacity decreases. Due to presence of high volumes of steel fiber, the fracture energy increases with increases in the a/d ratio.
[1]	RCC beam with a rectangular section and a T section.	1600 mm × 300 mm × 150 mm CFRP ropes were used for retrofitting and shear strengthening.	Three-point load	Compressive and tensile strengths of concrete were found to be 28.0 MPa and 2.70 MPa. The area of the CFRP rope was 28 mm^2 and the modulus of elasticity was 240 GPa.	CFRP ropes improve the structural performance of deep RC beams by converting brittle shear failure into ductile flexural failure.

In recent decades, bacterial mortar and concrete have also been used as sustainable materials for repairing microcracks and increasing the self-healing property of concrete. As it is organic material, its properties do not change with time, and thus it can be used for healing deep, internal microcracks. Cracks of more than 0.8 mm can be easily healed [24]. Bacteria that are rich in calcium are added to mortar or concrete during mixing. These bacteria precipitate calcium carbonate in the event that cracks emerge in the concrete, thus sealing the cracks and repairing them. Bacterial mortar or concrete has higher strength and durability than normal concrete. Kumari et al. (2017) [25] used *Bacilus Cohnii* (BC),

which can biologically increase durability and mechanical strength without producing any harmful gases. The encapsulation of the bacteria spores and nutrients by expanded perlite helps to heal the cracks, when 20% of the weight of the fine aggregates were replaced by expanded perlite [26]. Sierra et al. (2014) [26] used bio-based repaired mortar for the concrete beam. The flexural and compressive strength and dry shrinkage were measured. The performance of the bio-based repair mortar was studied through restrained shrinkage and pull-out tests [25]. Valdez Aguilar et al. (2021) [23] presented a detailed review on the various types of bacteria used for healing concrete and discussed the different concrete properties affected by the addition of bacteria. Vijay and Kunamineni et al. (2019) [27] used cultured bacillus subtilis in spore powder form and culture form in mortar concrete. From their experimental works, it was concluded that the compressive strength increases and also that evidence of aggregates in pores, which are responsible for the high concentration of Ca+ ion calcium silicate hydrate. In their study, Abo-El-Enein et al. (2019) [28] used microbes to precipitate the calcite by filling microcracks in order to increase compressive strength and decrease water absorption. The permeability of cracked concrete in wet–dry cycle conditions decreases because crack healing by calcium carbonate is precipitated by microbes [29]. Table 3 lists the types of bacteria, preparation curing specimens, test methods and major remarks based on the previous researchers on bacterial mortar and concrete. In case of bacterial mortar or concrete the bacteria used for the bio-precipitation process is an important stage.

Table 3. Review based on bacterial mortar and concrete.

Authors	Materials	Name of Bacteria	Preparation of Specimen and Curing	Test Method	Result and Discussion
[30]	Cement, sand, aggregate, bacteria liquid, cyclic-enriched ureolytic powder (CERUP), and activated compact denitrifying core (ACDC) granules.	*B. Cohni*	Specimens cured in water for 28 days.	Compressive strength, water absorption and recovery of water tightness.	Compressive strength increased by 25%, water absorption decreased, and due to the aerobic oxidation of organic carbon O_2 consumption by bacteria, the rebar corrosion was reduced.
[31]	Cement, sand, aggregate, with a ratio of 1:2.5 of water–bacterial liquid in a clay ball.	*Genus. Bacillus*	Specimens cured in water and a wet/dry cycle for 28 and 56 days.	Crack water permeability. Recovery of water tightness. Oxygen consumption measurements and ESEM analysis.	Crack permeability was lower than in normal concrete.
[27]	Portland slag cement and fine sand at a ratio of 1:6; bacterial solution w/c 0.55.	*B. Cohni*	Specimen cured in water for 28 days.	Standard consistency, setting time, cement soundness, compressive strength, sorptivity, drying shrinkage, microstructure, morphology, field emission scanning electron microscope (FESEM), and X-ray diffraction (XRD) techniques.	For 28 days, compressive strength increased by 49.8% and sorptivity decreased.
[28]	Portland cement, sand fly ash, silica fume, calcium lactate, calcium acetate, and encapsulated material.	*S. Pastteurii* and others ureolytic bacteria.	Specimen cured for 28 days.	Setting time of concrete, compressive strength, permeability, chloride ion permeability, and microstructure calcite.	Compressive strength increased and permeability decreased.
[32]	Cement, sand, bacterial liquid, encapsulated material.	*Ureolytic bacteria*	Specimen cured in buffer solution for 7 and 28 days.	Scanning electron microscope, compressive strength, permeability.	Permeability decrease.

Table 3. *Cont.*

Authors	Materials	Name of Bacteria	Preparation of Specimen and Curing	Test Method	Result and Discussion
[33]	Portland fly ash cement and sand at a ratio of 1:3; bacteria perlite, sodium silicate, water, calcium acetate, and yeast extract; w/c 0.5.	*B. Pseudoformu*	Specimens were cured in a controlled environment, then after demolding, the specimen was cured in water at 20 °C for 28 days. Cracked sample cured in a moist and humid environment for 165 days.	Surface water absorption and visualization of crack healing.	Water absorption decreases.
[29]	OPC, sand, and w/c 0.46 buffer solution.	*B. Pasturi*	Specimen cured in a humidity chamber with a relative humidity of 100% for 24 h. After demolding, the bacterial specimens were cured in buffer solution for 28 days.	Compressive strength and water absorption.	For 28 days, compressive strength increased by 33% and water absorption.
	Portland cement, sand, water, and encapsulated material.	*Ureolytic bacteria*	Specimens cured for 28, 60, 90, 365, and 730 days.	Compressive strength, flexural strength, and water absorption.	Compressive strength and flexural strength increased, construction cost increased, and maintenance cost decreased.
[34]	Portland cement, sand, water, and encapsulated material.	*Bacillus Cereus*	Specimen cured for 180 days.	Compressive and split tensile strength, ultrasonic pulse velocity and water absorption capacity.	Compressive and split tensile strengths were improved and reduced water absorption capacity.

Literature on based on recent advancements in non-destructive techniques have also been published: Adhikary et al. (2012) [35] three-dimensional finite element models were used in a parametric investigation, and their validity was checked against experimental data. The impacts of longitudinal and transverse reinforcement ratios, as well as the shear range-to-effective depth ratio, were investigated. Finally, empirical formulas were provided to predict the maximal resistance of RC beams at different loading rates as a function of the dynamic increase factor (DIF). Furthermore, IS 456 [36] incorporated non-destructive evaluation methods to continuously check concrete beams for deterioration or corrosion without endangering the structure. Bao et al. (2001) [37] advanced experimental methodologies that have been used to investigate the mechanical properties of concrete beams under various loading scenarios. These techniques include a variety of methods, such as measuring strain and stress distributions longitudinally along the beam with strain gauges and load cells. Roux et al. (2006) [38] adopted digital image correlation (DIC) for crack propagation analysis and surface deformation capture. Kim et al. (2003) [39] studied the matrix microcracks and fracture events of concrete using acoustic emission (AE) monitoring. By monitoring wave velocities and attenuation, ultrasonic testing (UT) is an important technique for assessing the integrity and homogeneity of concrete beams. Moreover, Hafezolghorani, Milad, et al (2017) [40] incorporated fiber optic sensors facilitate the tracking of variations in temperature and moisture penetration in concrete beams. Yehia et al. (2007) [41] proposed that without producing any structural damage, non-destructive evaluation (NDE) techniques are essential for monitoring the performance and condition of concrete beams. The authors of [18,42] used ground-penetrating radar (GPR) to find corrosion, cavities, and cracks in concrete buildings. Villain et al. (2012) [43] created a 2D data fusion model using GPR and developed an eco-friendly impact approach to forecast

the service life of concrete structures in maritime environments. Bogas et al. (2013) [44] used ultrasonic pulse velocity (UPV) testing measures the propagation of ultrasonic waves and provided a dependable way to evaluate the homogeneity and quality of concrete. Tran et al. (2017) [45] noted that the use of thermal imaging to detect thermal abnormalities potentially containing moisture intrusion, delamination, or other flaws in concrete beams has shown promise. Murad et al. (2021) [46] suggested acoustic emission techniques for the assessment of concrete dams. These non-destructive evaluations collectively contribute to a comprehensive understanding of the conditions and performances of concrete beams, facilitating timely maintenance and ensuring long-term structural reliability.

Other previous studies related to the effects of microstructures in influencing crack propagation paths and ultimately impacting material behavior under loads are described as follows. Xie et al. (200) [47] suggested that microstructure analysis plays a critical role in identifying the fracture properties of cementitious specimens. Li et al. (1986) and Wahab et al. (2012) [48,49] used the technique for examining the fine details of fracture surfaces and demonstrated that the fundamental principles driving crack propagation are microstructure-related [50,51]. Furthermore, Devi at al. (2022) [50] carried out the three-dimensional reconstruction of microstructures by sophisticated imaging modalities like focused ion beam-scanning electron microscopy (FIB-SEM) and X-ray microtomography (XMT), which shed light on the spatial distribution of phases and interfaces inside the material. Landis and Keane et al. (2010) [51] demonstrated that fracture properties, such as crack morphology, crack route, and the existence of microcracks and flaws on the fracture surface of cement specimens, can be discovered through microstructure analysis. Kotula et al. (2014) [52] studied the behavior of the material under loads and its ability to withstand the propagation of cracks by establishing a correlation between these observations and mechanical characteristics including tensile strength, fracture toughness, and energy dissipation.

Furthermore, Lange et al. [53] analyzed microstructural aids in identifying important microstructural characteristics, such as aggregate presence, porosity distribution, and interfacial bonding between phases, that affect fracture behavior. Launey and Ritchie (2009) [54] observed that knowledge obtained from a study on fracture surface microstructure has important ramifications for material design and performance optimization. Through comprehending the ways in which microstructural characteristics impact fracture patterns, scientists can devise methods to improve the mechanical characteristics and service lives of cementitious materials.

Contribution of Work

From this literature review it can be seen that no comparison had been conducted on the cement, bacterial mortar, and commonly used adhesive materials. In the present experimental and numerical investigations, the effects of ultimate flexural loads on concrete beams with different width-to-depth ratios of the notches under a three-point loading test were studied. Further, the flexural performance of notched concrete beams repaired with the three repair materials (cement mortar, bacterial mortar, and adhesive) was also investigated. Consequently, a comparative study was carried out between the experimental and numerical results in order to study the performance of these repair materials for the concrete structures. Also, the application of bacterial mortar as a repair material was studied. A concrete damage plasticity (CDP) model was used for finite element numerical analysis of beams. Additionally, a linear regression model was used to predict the ultimate load values at a notch width interval of 5 mm up to a maximum notch width of 100 mm.

2. Experimental Study

Concrete beam specimens were fabricated with a specific composition for each constituent material for M40 grade, as per IS 10262:2019 [55]. The strength of pozzolana Portland cement (PPC) with a standard consistency 31.5% and a specific gravity is 3.14, and Narmada River sand acts as a fine aggregate that remains in confining zone II of

IS 383:2016 [55], and maximum size of 20 mm coarse aggregates were used. The SIKA plasticizer was used as an admixture. The mix proportion cement: fine aggregates: coarse aggregates adopted was 1:1.52:2.72 with a water-cement ratio 0.40 and admixture 1.1% by weight of cement. A cement content of 445 kg/m^3 and workability with a 0.85 compaction factor were used. The fresh concrete mixed workability as per the designed mix proportions was first investigated, a further total 21 specimens of concrete beams sized 100 mm × 100 mm × 500 mm were cast. The solid concrete beam specimens were cast as shown in Figure 2a. The beam specimens were removed from their molds 24 h after casting and then cured in water at room temperature for 28 days. Further, the required size of the rectangular-shaped notch was marked on the middle span of the concrete beam on the tension side (bottom face) after 28 days curing the hardened concrete beam, as shown in Figure 2b. The notch was cut with the help of grinder with a circular blade. The notch was cut from one side, and then we moved slowly cut-by-cut to the other side along the width of the beam specimen. Precautions were taken to prevent the incorrect cutting of a notch and to cut the desired size of notch without damaging the specimens. The notch was cut three hours before testing the specimens. The notch was considered suitable to simulate failure or crack or defect in a beam that were necessary to repair. The different width-to-depth ratios 0.33, 1.66, and 3.33 of the notches were considered in the present investigation. Rectangular notches with widths of 10 mm, 50 mm, and 100 mm and constant depths of 30 mm at the center of the tension side of the beam were considered.

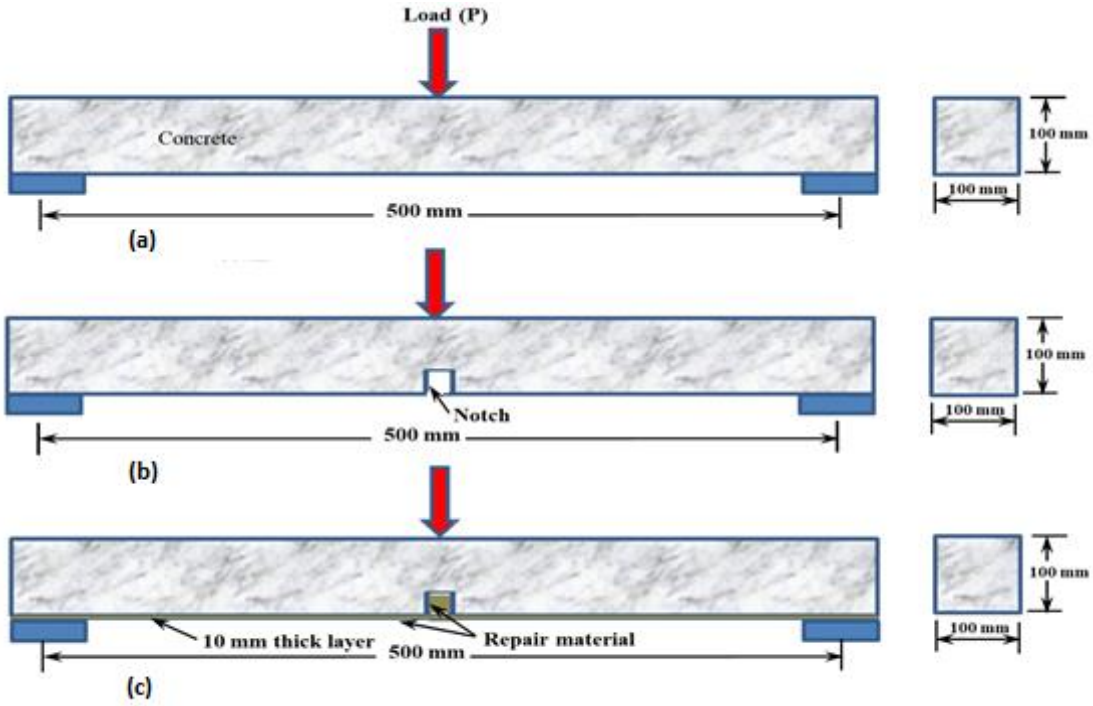

Figure 2. Concrete beam specimens: (**a**) three-point load testing of solid beam; (**b**) three-point load testing of notched beam; (**c**) three-point load testing of notched beams repaired with respective materials.

Further, in order to study the effects of the three repairing materials, i.e., cement mortar, bacterial mortar, and adhesive (Sikadur-31), the notches were filled with repairing materials and a 10 mm thick layer of material was placed on the tension side, as shown in Figure 2c. The effect of the repairing material on the flexural strengthening resistance of concrete beam was studied. In the case of cement mortar, a cement-to-sand ratio of 1:3 and a water-to-cement ratio of 0.50 was used and cured for 28 days.

In case of bacterial mortar, *Bacillus cohnii* (MTTCC3616) was procured from IMTECH, CSIR Labs Chandigarh, India. All revival cells were incubated in calcium precipitate culture for 72 h using a shake flask incubator at 37 °C and 150 rpm, as shown in Figure 3. After

incubation time, the culture was mixed with cement and sand at a 1:3 proportion, and the culture-to-cement ratio was 0.5. Figure 3 depicts the step-by-step procedure for preparing the bacterial mortar and its use as a repair material. The bacterial cement mortar specimens were prepared similarly to the above method. The specimens were cured in water with a 0.1 Mol calcium lactate powder solution in order to provide the external calcium resource for the bacteria used in the mortar. The third repair material, thixotropic epoxy adhesive, was used, and after its application, it was left to dry for at least 15 days at room temperature. In order to eliminate the uncertainty of the concrete material, three concrete beams were cast for each solid beam, notched beam, and beam with repair material.



(**a**)

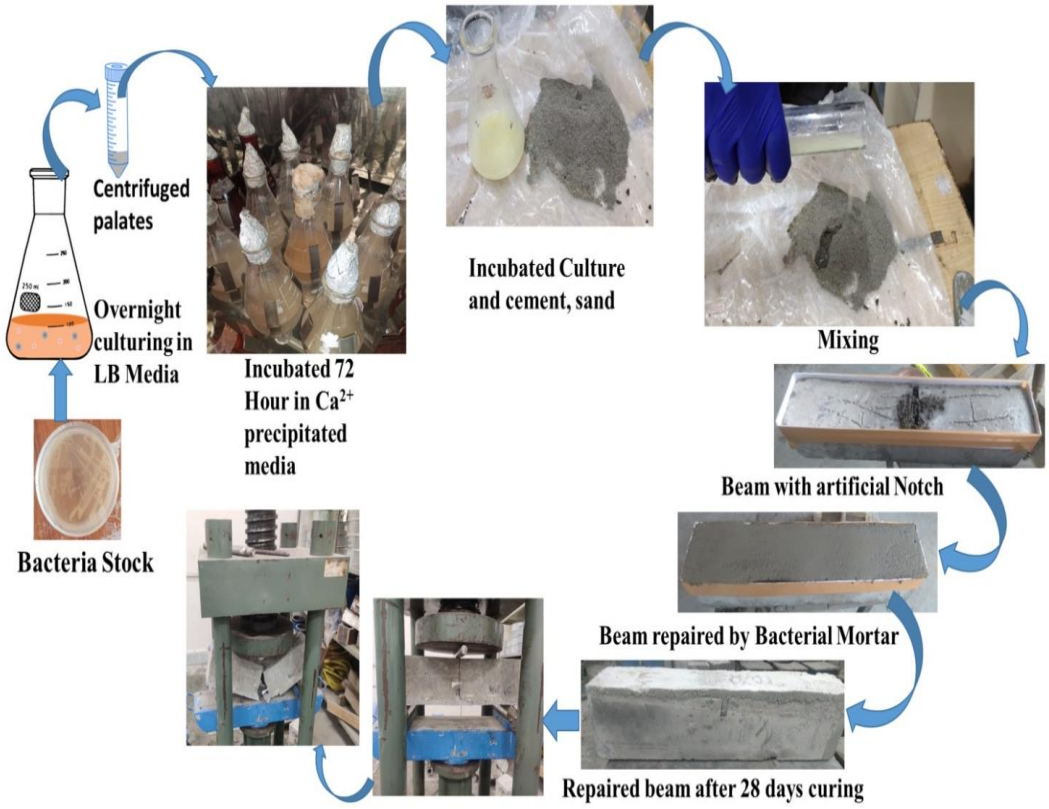

(**b**)

Figure 3. Bacterial mortar: (**a**) bacteria kept in a shake flask incubator; (**b**) bacterial mortar preparation process.

The casting and testing procedure of the beam indicated 4 (a-g). The concrete beam specimens were mounted and simply supported on a servo-hydraulic testing machine, and single point load was applied at the middle of the length (three-point flexural test) of the concrete beam specimen, as shown in Figure 4e. The reaction was carried out by the two roller-supports near the ends of the concrete beam specimens. The strength tests on the concrete beam specimens were conducted as per the Indian Standard—IS 456:1959 [36]. The values for the ultimate flexural load for each specimen were recorded, and flexural behavior was studied, as shown in Figure 4f.



(**a**)



(**b**)



(**c**)



(**d**)



(**e**)



(**f**)

Figure 4. *Cont.*



(**g**)

Figure 4. Experimental study of the beam: (**a**) casting of solid concrete beam specimens; (**b**) notch concrete beam; (**c**) notched beam repaired using bacterial mortar; (**d**) notched beam repaired using adhesive; (**e**) three-point flexural test on beam specimen; (**f**) flexural failure behavior of notched beams; (**g**) flexural failure behavior of repaired notched beams.

3. Numerical Study

Further, in the present work, a numerical study was also carried out. The numerical study is a more efficient and economical tool as compared to the experimental study for structural analysis and engineering research. Thus, numerical studies can capture complex damage behavior accurately. The finite element modeling of beams was carried out using the commercial software ABAQUS (Abaqus 6.21-1, Simulia, Dassault Systemes, Paris, France) [56]. Concrete was modeled using the smeared crack concrete model and the concrete damage plasticity (CDP) model. The purpose of the model was to calculate beam performance during experimental testing. In the present study, the concrete damage plasticity (CDP) model [47–50] was used. This model is based on the proposed models by Lee and Fenves (2018) [57] and Lubliner et al. (1989) [58], which can simulate the tensile cracking and compressive crushing of concrete materials while considering the isotropic elastic damage and plastic behaviors of the materials. The CDP model is used for applications where concrete is subjected to arbitrary loading circumstances, such as cyclic loading, and is predicated on the idea of scalar (isotropic) damage. The model accounts for the plastic straining-induced deterioration of elastic stiffness in both tension and compression. The effects of stiffness recovery during cyclic loading are also taken into account. The material properties, such as elastic modulus, Poisson's ratio, and damage parameters must be specified [45].

3.1. Validation of the Numerical Model

The present numerical model was validated using the published results in the literature. Table 4 shows the comparison of the three-point flexural test maximum failure load with published results and represents a numerical study. The percentages of difference are negligible and good agreement is achieved between both set of results.

Table 4. Verification of the numerical results.

References	Material Properties	Dimensions	Maximum Failure Load (N)		% Difference
			Published Results	Present Study Results	
[52]	E= 32.89 GPa and f_{ck} = 41.2 MPa	500 mm × 100 mm × 100 mm, notch 10 mm × 10 mm × 100 mm.	6933.3	6606	4.72
[53]	f_{ck} = 38.24 MPa	L = 1200 mm, d = 200 and b = 100 mm.	11,200	10,770	3.83
	f_{ck} = 54 MPa, f_{tk} = 3.16	L = 1400 mm, d = 230 mm and b = 140 mm.	16,000	15,963	0.23

3.2. Present Numerical Study

Further, the concrete beam was modeled using an eight-node linear brick C3D8R element with six faces and reduced integration with an hourglass control, as shown in Figure 5. The boundary condition was designated as a simply supported beam with two hinged supports at a distance of 50 mm from each end of the beam and was modeled. The central point load was applied at a reference point on the middle top of the beam. Based on the convergence study, a 20 mm sized mesh was utilized, and a fine mesh of 10 mm was used near the notch section. All material properties in the CDP model for the M40-grade concrete were adapted from [14,59]. The mechanical properties for the M40-grade concrete are given in Table 5, and Table 6 shows the mechanical properties of the repairing materials. In total, 21 FE concrete beam models were simulated and compared with the experimental results for solid, notched, and repaired beams.

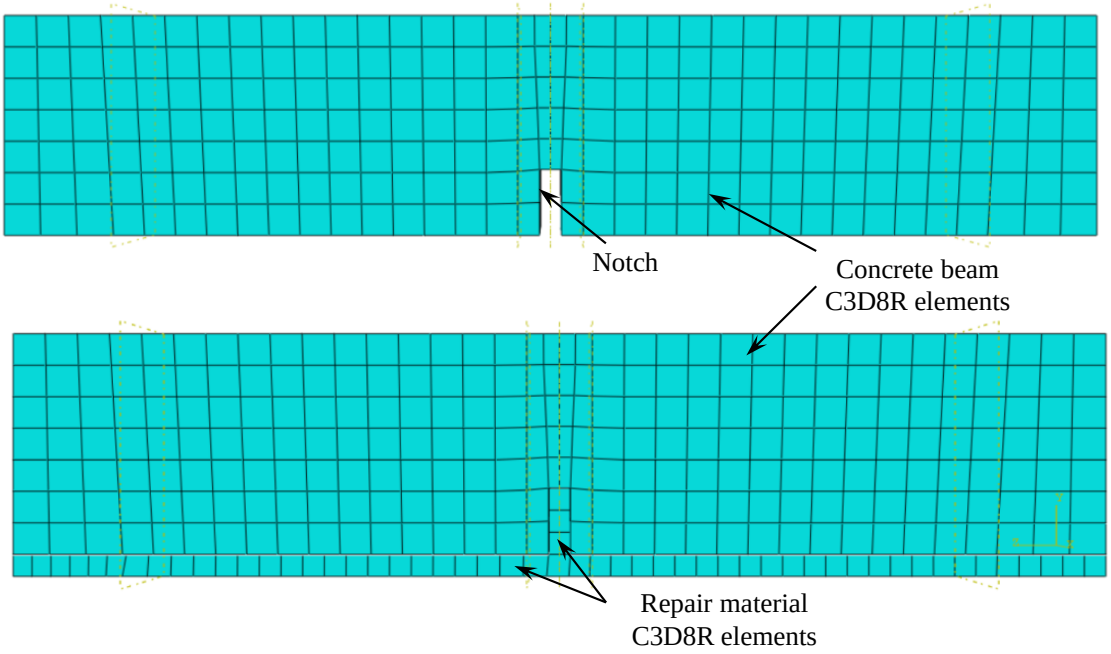

Figure 5. Numerical models.

Table 5. Mechanical properties for M40-grade concrete.

Material	f_{ck} (MPa)	f_{tk} (MPa)	Modulus of Elasticity (MPa)	Density (kg/m^3)	Poisson's Ratio	Dilation Angle	Viscosity
Concrete	40	4.6	32,890	2400	0.2	31°	0.00001

Table 6. Mechanical properties of repairing materials.

Repairing Material	Density	Compressive Strength (N/mm^2)	Modulus of Elasticity (MPa)	Poisson's Ratio
Cement mortar	2200 (kg/m^3)	36.22 in 28 days	14,108.08 [60]	0.2
Bacterial mortar	2200 (kg/m^3)	63.43 in 28 days	30,387.43 [60]	0.2
Adhesive	1.8 (kg/lit)	65 in 15 days	11,000 [61]	0.25

4. Results and Discussion

In the current experimental and numerical investigations, concrete beams with different width-to-depth ratios of the notches on its ultimate flexural load were studied. Further, the flexural performance of repaired notched concrete beams using the three repair materials, namely cement mortar, bacterial mortar, and adhesive, was also investigated. The

experiment's validity and accuracy are demonstrated by the strong agreement between the numerical and the experimental observations.

4.1. Effect of Notching

The effect of the different width-to-depth ratios of 0.33, 1.66, and 3.33 of the notches were considered in the present investigation. The rectangular notches had widths of 10 mm, 50 mm, and 100 mm with a constant depth of 30 mm and were located at the center of the tension side of the beams. Figure 6 shows the ultimate flexural load versus the displacement behavior of the solid beams and the notched beams with different notch sizes. According to the experimental study, in the case of the solid beam, the ultimate load capacity was 12.33 kN, and according to the numerical study, the load obtained was 10.09 kN. Thus, the percentage difference in both the experimental and numerical studies is 0.65–22.20%. Figure 7 shows the comparison of the ultimate loads of the experimental study and the numerical study. Thus, the CDP model can accurately simulate the flexural behavior of the concrete beam.

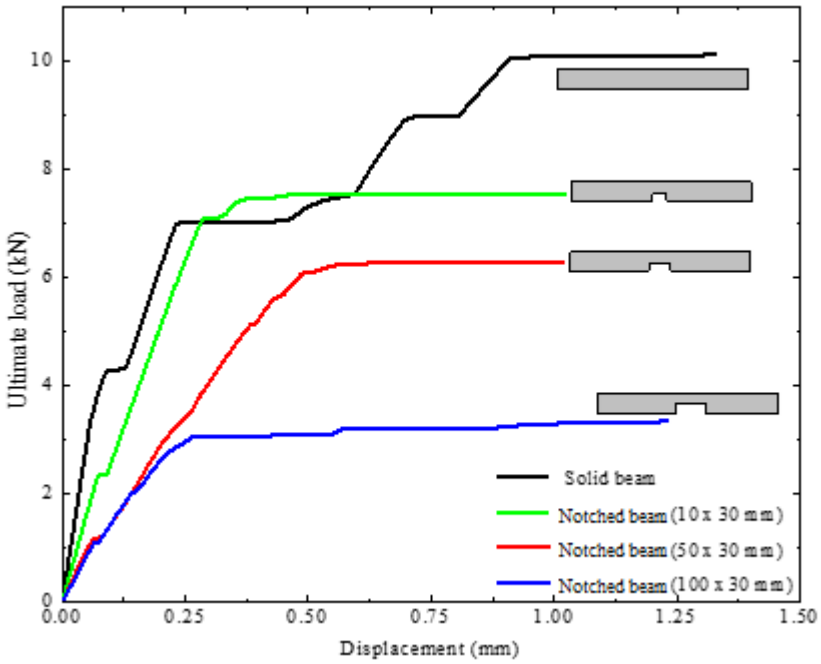

Figure 6. Ultimate load–displacement behavior for solid concrete beam; (10 × 30 mm) notched concrete beam; (50 × 30 mm) notched concrete beam; (100 × 30 mm) notched concrete beam.

The notched beam with a notch size of 10 × 30 mm had a 0.6% reduction in volume as compared to the solid beam, and the percentage reduction in load carrying capacity was observed to be 41.20%; this was similar to the case of the notched beam with a notch size of 50 × 30 mm, which saw 3% reduction in volume as compared to the solid beam, and the percentage reduction in load carrying capacity was observed to be 50.04%. Further, the notched beam with a notch size 100 × 30 mm saw a 6.0% reduction in volume as compared to the solid beam, and the percentage reduction in load carrying capacity was observed to be 67.56%. It can be observed that as the notch size increased the ultimate load carrying capacity of beam was reduced. Thus, the defects and cracks reduce the load performance capacity of the beam. Thus, in the case of the notched beam, the ligament area can be enhanced by decreasing the width-to-depth ratio of the notches, which increases the resistance to flexural damage and enhances the flexural capacity of the concrete beam.

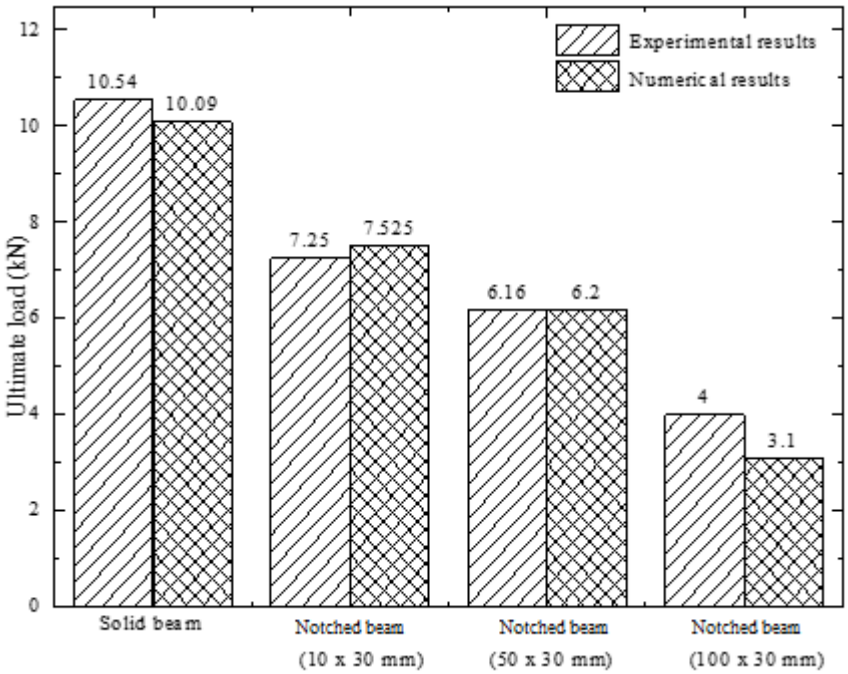

Figure 7. Comparison of ultimate load between the experimental and numerical studies.

The relationship between ultimate load carrying capacity and concrete beams was uncovered based on the proposed experimental and numerical results. Almusallam et al. (1997), Murad et al. (2021), and Zhong et al. (2021) also predicated the load capacity of the concrete beams [62,63]. Further, the experimental and numerical results were used for applying a prediction model linear regression (LR) for precise notch width for a 30 mm constant depth. To apply the LR model, first, the existing experimental and numerical ultimate load values for notch widths (10 mm, 50 mm, and 100 mm) were used to validate the LR regression model. In the second stage, the LR model was used to predict the ultimate load values at a notch width interval of 5 mm up to maximum notch width of 100 mm, as shown in Figure 8. The LR mathematical model is defined as follows:

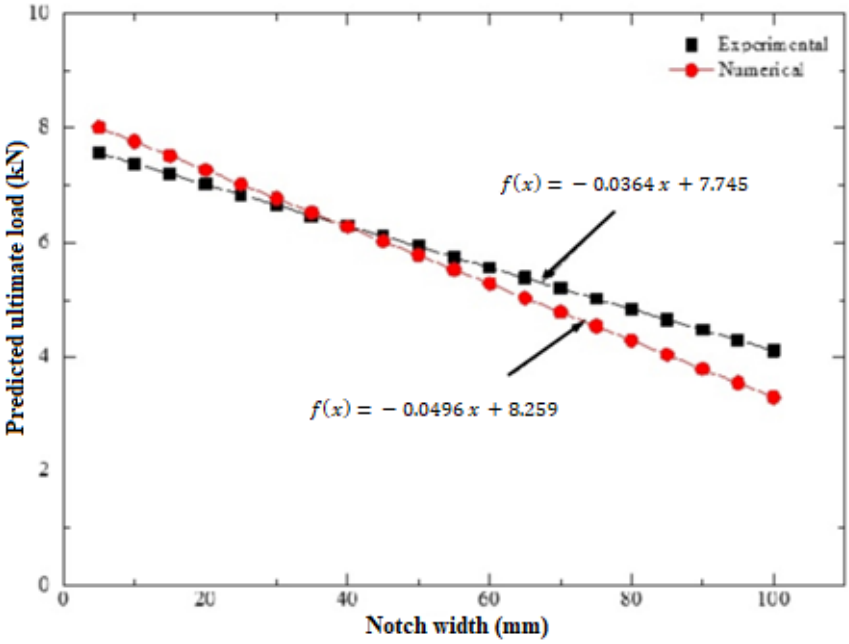

Figure 8. Predicted experimental and numerical results for notched beams.

Where p_1 and p_2 are linear regression coefficients. The predicated coefficients of the proposed linear regression model are presented in Table 7. It can be seen that the correlation coefficient R^2 with experimental and numerical results shows a difference of nearly 1.12%. The root mean square errors (RMSE) for experimental and numerical results are 0.288 and 0.522, respectively.

Table 7. Parametric values of the prediction model.

Parameters	Experimental	Numerical
Coefficients	$p_1 = -0.0364$, $p_2 = 7.745$	$p_1 = -0.0496$, $p_2 = 8.259$
R^2	0.984	0.973
RMSE	0.288	0.522

4.2. Effect of Repairing Materials

The flexural load carrying capacity of notched beams repaired with the three repair materials, i.e., cement mortar, bacterial mortar, and adhesive, was also investigated. In this case, the notch beam with a notch size of 10 × 30 mm was considered and repaired with cement mortar, bacterial mortar, and adhesive. After the repair, the ultimate flexural load of the beam was determined experimentally and also numerically. Figure 9 illustrates the ultimate load–displacement curve for the repaired concrete beam with all three repair materials under consideration. It can be observed that the ultimate load capacity for the repaired beam was increased as compared to the notched beam.

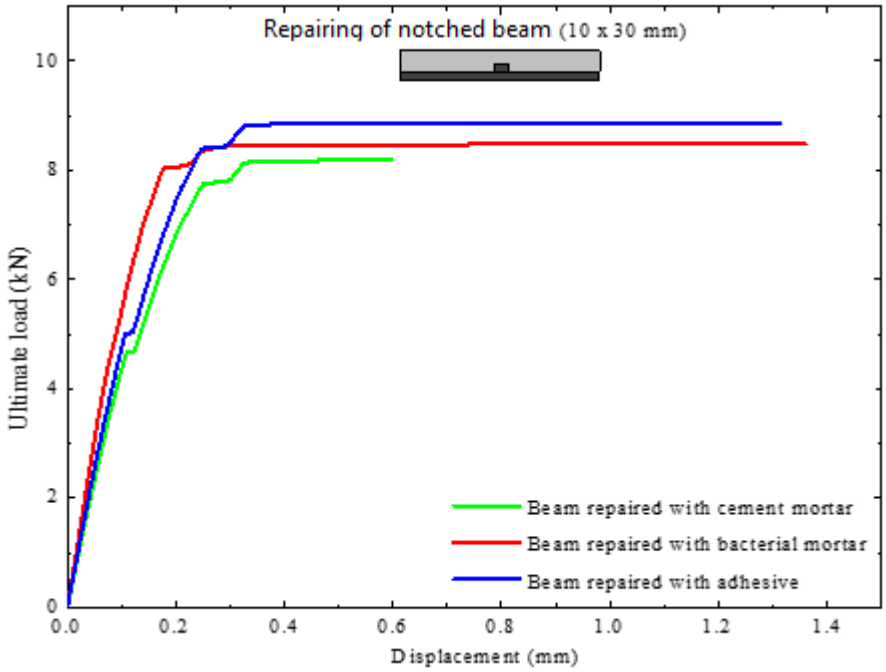

Figure 9. Ultimate load–displacement behavior for repaired concrete beam.

In the case of cement mortar, the ultimate load was observed to be 7.60 kN as compared to the notched beam with an ultimate load of 7.25 kN. The maximum ultimate load in case of notched beam that was repaired using adhesive was increased to 12.24 kN. Figure 10 shows the comparison of the ultimate load in repaired beams for different materials and also a comparison between the experimental and numerical results. It can be seen that the CDP model can explicitly simulate the repairing material. The numerical result depends on the precision of the input data of the material. Figure 11 shows the numerical simulation results for the repaired beam. The adhesive repair material initially provides more load

capacity, but it is costly, and the performance also decreases with respect to time and variation in the materials' properties due to environmental conditions. The procedure for using the adhesive material is easy as compared to the cement and the bacterial mortars. The ultimate load for the bacterial mortar is 7.3% more than that for the cement mortar. Thus, as compared to the cement mortar, the performance of the bacterial mortar was better in terms of the ultimate load. The bacterial mortar was more sustainable and more durable as a repair material for concrete structures.

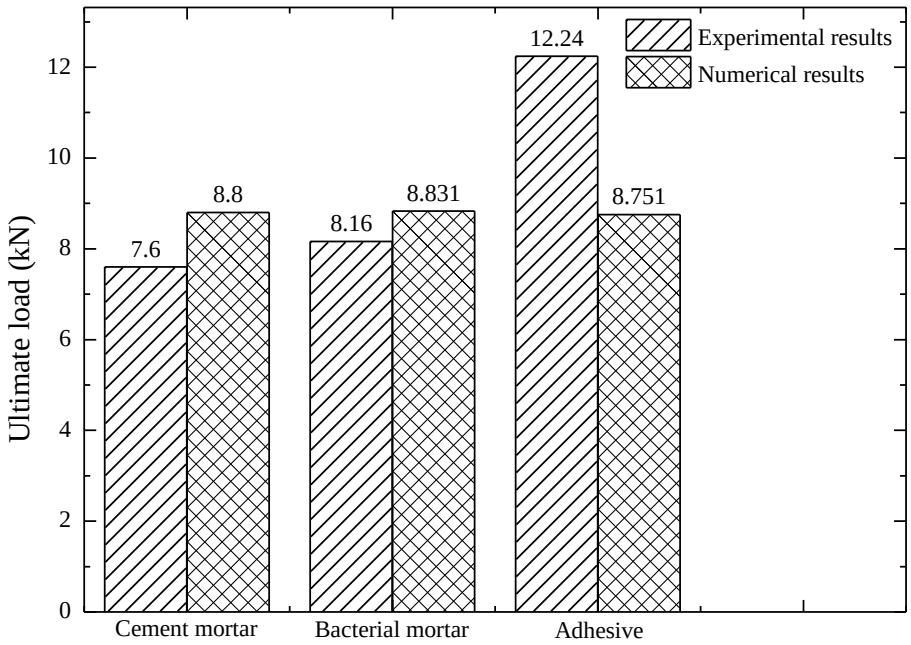

Figure 10. Comparison of ultimate loads in repaired beams for different materials.

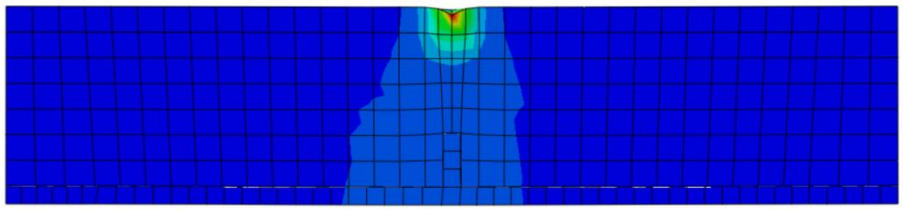

(**a**) Deflected shape.

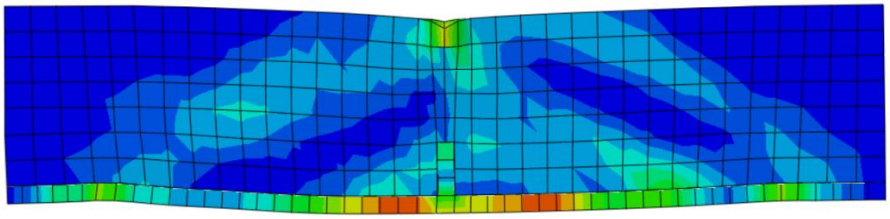

(**b**) Flexural failure behavior.

Figure 11. Simulation behavior of repaired beam: (**a**) deflected shape of repaired beam with crack path, and the contour color shows the crack pattern failure; (**b**) flexural stress of repaired beam.

5. Conclusions

In the current experimental and numerical investigations, the effect of the ultimate flexural load on concrete beams with different width-to-depth notch ratios under three-

point loading tests was studied. Further, the flexural performance of repaired notched concrete beams using the three repair materials, namely cement mortar, bacterial mortar, and adhesive, was also investigated. Consequently, a comparative study of the experimental and numerical results was carried out. The following conclusions can be summarized as follows:

1. There is an excellent correlation between the experimental and finite element numerical results at every loading stage up to the point of failure to predicate the flexural behavior of the concrete beam. Additionally, the FE numerical platform can overcome the drawbacks of experimental testing.
2. The differences in numerical and experimental results ranged from 0.65% to 22.20% for the ultimate load carrying capacity.
3. As the notch size increases, the ultimate load carrying capacity of the beam is reduced. The notch volume ranged from 0.6 to 6% with a percentage reduction in load carrying capacity in the range of 41.20–67.56%.
4. A linear regression (LR) model was proposed to predict the ultimate load values at a notch width interval of 5 mm up to maximum notch width of 100 mm. It can be observed that the ultimate load capacity of the repaired beams was increased when compared to the notched beams with all three repairing materials under consideration.
5. It can be seen that the correlation coefficient with experimental and numerical results shows a difference of nearly 1.12%. The root mean square errors (RMSE) for the experimental and numerical results are 0.288 and 0.522, respectively.
6. The maximum ultimate load was increased in case of the notched beam repaired using adhesive. Additionally, the FE numerical platform can be used to simulate the repair materials and to study their performance. As compared to the cement mortar, the performance of the bacterial mortar was better in terms of the ultimate load. The bacterial mortar is more sustainable and more durable as a repair material for concrete structures.
7. The selection of any repair and/or strengthening material depends on repair time, localized changes in the stiffness of the member, strength, ductility, durability, cost, and work safety.

Author Contributions: W.K.: investigation, methodology, validation, visualization, writing—original draft. S.A.: conceptualization, writing—review and editing. A.R.: conceptualization, methodology, writing—review and editing. A.B.: conceptualization, writing—review and editing. All authors have read and agreed to the published version of the manuscript.

Funding: This research received no external funding.

Institutional Review Board Statement: Not applicable.

Data Availability Statement: All data is available on genuine request.

Acknowledgments: Waseem Khan acknowledge UGC New Delhi for MANF fellowship. W K is grateful to UGC New Delhi (F1-17.1/201718-MANF-2017-18-MAD-79399) for financial assistance.

Conflicts of Interest: The author declares no conflicts of interest.

List of Abbreviations

AE	Acoustic emission
AFM	Atomic force microscopy
B. Pasturi	*Bacillus Pastutri*
CDP	Concrete damage plasticity
CFRP	Carbone fiber-reinforced polymer
DIF	Dynamic increase factor
FESEM	Field emission scanning electron microscopy
FIB	Focused ion beam
FRP	Fiber-reinforced polymer

GPR	Ground penetrating radar
HPC	High performance concrete
IMTECH, CSIR	Institute of Microbial Technology, Council of Scientific and Industrial Research
IS	Indian Standard
LR	Linear regression
MTTCC3616	Microbial Type Culture Collection and Gene Bank
NDE	Non-destructive evaluation
NDT	Non-destructive testing
OPC	Ordinary Portland cement
PPC	Pozzolana Portland cement
R^2	Correlation coefficient
RCC	Reinforce cement concrete
RMSE	Root mean square errors
SEM	Scanning electron microscopy
SFRP	Steel fiber-reinforced polymer
SMA	Shape memory alloy
TEM	Transmission electron microscopy
UPA	Ultra-sonic pulse velocity
UT	Ultra-sonic testing
XFEM	Extended finite element method
XMT	X-ray microtomography
XRD	Extended finite element method

List of Notations

$\mu_{\text{Foamed Concrete}}$	Poisson ratio of foamed concrete
μ_{Adhesive}	Poisson ratio of adhesive
μ_{CFRP}	Poisson ratio of CFRP
$E_{\text{Foamed Concrete}}$	Modulus foamed concrete
$E_{A\text{dhesive}}$	Modulus of elasticity of adhesive
E_{C}	Modulus of elasticity of concrete
E_{CFRP}	Modulus of elasticity of CFRP
f_{ck}	Compressive strength of concrete
f_{tk}	Tensile strength of concrete
MI_{Concrete}	Moment of inertia of concrete
w/c	Water-to-cement ratio
ρ_{concrete}	Density of concrete
$\rho_{\text{foamed concrete}}$	Density of foamed concrete
φ	Angle of repose

References

1. Luo, M.; Qian, C.; Li, R. Factors affecting crack repairing capacity of bacteria-based self-healing concrete. *Constr. Build. Mater.* **2015**, *87*, 1–17. [CrossRef]
2. Obaid, W.A.; AL-asadi, A.K.; Shaia, H. Repair and strengthening of concrete beam materials using different CFRP laminates configuration. *Mater. Today Proc.* **2022**, *49*, 2806–2810. [CrossRef]
3. Hassan, R.F.; Latief, A.F. Repairing and strengthening techniques of RC beams: A review, 3rd International Conference for Civil Engineering Science (ICCES 2023). *IOP Conf. Ser. Earth Environ. Sci.* **2023**, *1232*, 012032. [CrossRef]
4. Martinola, G.; Meda, A.; Plizzari, G.A.; Rinaldi, Z. Strengthening and repair of RC beams with fiber reinforced concrete. *Cem. Concr. Compos.* **2010**, *32*, 731–739. [CrossRef]
5. Pešić, N.; Pilakoutas, K. Flexural analysis and design of reinforced concrete beams with externally bonded FRP reinforcement. *Mater. Struct./Mater. Constr.* **2005**, *38*, 183–192. [CrossRef]
6. Balsamo, A.; Nardone, F.; Iovinella, I.; Ceroni, F.; Pecce, M. Flexural strengthening of concrete beams with EB-FRP, SRP and SRCM: Experimental investigation. *Compos. Part B Eng.* **2013**, *46*, 91–101. [CrossRef]
7. Słowik, M. The analysis of failure in concrete and reinforced concrete beams with different reinforcement ratio. *Arch. Appl. Mech.* **2019**, *89*, 885–895. [CrossRef]
8. Sharaky, I.A.; Ahmed, S.E.; Alharthi, Y.M. Flexural response and failure analysis of solid and hollow core concrete beams with additional opening at different locations. *Materials* **2021**, *14*, 7203. [CrossRef]

9. Dong, Y.; Ming, Z.; Ansari, F. Failure characteristics of reinforced concrete beams repaired with CFRP composites. In Proceedings of the Third International Conference on Composites in Infrastructure (ICCI'02), Francisco, CA, USA, 10–12 June 2002; pp. 51–65.
10. Rahim, N.I.; Mohammed, B.S.; Al-Fakih, A.; Wahab, M.M.A.; Liew, M.S.; Anwar, A.; Amran, Y.H.M. Strengthening the structural behavior of web openings in RC deep beam using CFRP. *Materials* **2020**, *13*, 2804. [CrossRef]
11. Maraq, M.A.A.; Tayeh, B.A.; Ziara, M.M.; Alyousef, R. Flexural behavior of RC beams strengthened with steel wire mesh and self-compacting concrete jacketing—Experimental investigation and test results. *J. Mater. Res. Technol.* **2021**, *10*, 1002–1019. [CrossRef]
12. Chalioris, C.E.; Pourzitidis, C.N. Rehabilitation of shear-damaged reinforced concrete beams using self-compacting concrete jacketing. *ISRN Civ. Eng.* **2012**, *2012*, 816107. [CrossRef]
13. Mostofinejad, D.; Shameli, S.M. Externally bonded reinforcement in grooves (EBRIG) technique to postpone debonding of FRP sheets in strengthened concrete beams. *Constr. Build. Mater.* **2013**, *38*, 751–758. [CrossRef]
14. Sirisonthi, A.; Julphunthong, P.; Joyklad, P.; Suparp, S.; Ali, N.; Javid, M.A.; Chaiyasarn, K.; Hussain, Q. Structural behavior of large-scale hollow section RC beams and strength enhancement using carbon fiber reinforced polymer (CFRP) composites. *Polymers* **2022**, *14*, 158. [CrossRef] [PubMed]
15. Grégoire, D.; Rojas-Solano, L.B.; Pijaudier-Cabot, G. Failure and size effect for notched and unnotched concrete beams. *Int. J. Numer. Anal. Methods Geomech.* **2013**, *37*, 1434–1452. [CrossRef]
16. Ameli, Z.; Rahman, M.M.; Carloni, C. Largest experimental investigation on size effect of concrete notched beams. *J. Eng. Mech. ASCE* **2023**, *150*. [CrossRef]
17. Nunes, L.C.S.; Reis, J.M.L. Experimental investigation of mixed-mode-I/II fracture in polymer mortars using digital image correlation method. *Lat. Am. J. Solids Struct.* **2014**, *11*, 330–343. [CrossRef]
18. Huang, X.; Wang, J.; Zhang, F.; Niu, S.; Ding, J. An experimental investigation on the failure behavior of a notched concrete beam strengthened with carbon fiber-reinforced polymer. *Int. J. Polym. Sci.* **2015**, *2015*, 729320. [CrossRef]
19. Kadela, M.; Cińcio, A.; Kozlowski, M. Degradation analysis of notched foam concrete beam. *Appl. Mech. Mater.* **2015**, *797*, 96–100. [CrossRef]
20. Rahman, N.A.; Jaini, Z.M.; Rahim, N.A.A.; Razak, S.A.A. An experimental study on the fracture energy of foamed concrete using V-notched beams. In *InCIEC 2014*; Hassan, R., Yusoff, M., Alisibramulisi, A., Mohd Amin, N., Ismail, Z., Eds.; Springer: Singapore, 2015. [CrossRef]
21. Benarbia, D.; Benguediab, M. Propagation of cracks in reinforced concrete beams cracked and repaired by composite materials. *Mech. Mech. Eng.* **2017**, *21*, 591–601.
22. Lacidogna, G.; Piana, G.; Accornero, F.; Carpinteri, A. Experimental investigation on crack growth in pre-notched concrete beams. *Proceedings* **2018**, *2*, 429. [CrossRef]
23. Valdez Aguilar, J.; Juárez-Alvarado, C.A.; Mendoza-Rangel, J.M.; Terán-Torres, B.T. Effect of the notch-to-depth ratio on the post-cracking behavior of steel-fiber-reinforced concrete. *Materials* **2021**, *14*, 445. [CrossRef] [PubMed]
24. Vijay, K.; Murmu, M.; Deo, S.V. Bacteria based self healing concrete–A review. *Constr. Build. Mater* **2017**, *152*, 1008–1014. [CrossRef]
25. Kumari, C.; Das, B.; Jayabalan, R.; Davis, R.; Sarkar, P. Effect of nonureolytic bacteria on engineering properties of cement mortar. *J. Mater. Civ. Eng. ASCE* **2017**, *29*, 06016024. [CrossRef]
26. Sierra-Beltran, M.G.; Jonkers, H.M.; Schlangen, E. Characterization of sustainable bio-based mortar for concrete repair. *Constr. Build. Mater.* **2014**, *67 Pt C*, 344–352. [CrossRef]
27. Vijay, K.; Murmu, M. Effect of calcium lactate on compressive strength and self-healing of cracks in microbial concrete. *Front. Struct. Civ. Eng.* **2019**, *13*, 515–525. [CrossRef]
28. Abo-El-Enein, S.A.; Ali, A.H.; Talkhan, F.N.; Abdel-Gawwad, H.A. Application of microbial bio cementation to improve the physical mechanical properties of cement mortar. *HBRC J.* **2019**, *9*, 36–40. [CrossRef]
29. De Belie, N. Application of bacteria in concrete: A critical evaluation of the current status. *RILEM Tech. Lett.* **2016**, *1*, 56–61. [CrossRef]
30. Tziviloglou, E.; Wiktor, V.; Jonkers, H.M.; Schlangen, E. Bacteria-based self-healing concrete to increase liquid tightness of cracks. *Constr. Build. Mater.* **2016**, *122*, 118–125. [CrossRef]
31. Gupta, S.; Dai, P.S.; Wei, K.H. Autonomous healing in concrete by bio-based healing agents—A review. *Constr. Build. Mater.* **2017**, *146*, 419–428. [CrossRef]
32. Alazhari, M.; Sharma, T.; Heath, A.; Cooper, R.; Paine, K. Application of expanded perlite encapsulated bacteria and growth media for self-healing concrete. *Constr. Build. Mater.* **2018**, *160*, 610–619. [CrossRef]
33. Morsali, S.; Isildar, G.Y.; Zargari, Z.H.; Tahni, A. The application of bacteria as a main factor in self-healing concrete technology. *J. Build. Pathol. Rehabil.* **2019**, *4*, 7. [CrossRef]
34. Priyom, S.N.; Islam, M.M.; Islam, G.M.S.; Islam, M.S.; Rahman, M.A.; Zawad, M.F.S.; Shumi, W. Efficacy of Bacillus Cereus Bacteria in Improving Concrete Properties through Bio-precipitation. *Iran. J. Sci. Technol. Trans. Civ. Eng.* **2023**, *47*, 3309–3320. [CrossRef]
35. Adhikary, S.; Li, B.; Fujikake, K. Dynamic behavior of reinforced concrete beams under varying rates of concentrated loading. *Int. J. Impact Eng.* **2012**, *47*, 24–38. [CrossRef]
36. *IS456-2000*; Code of Practice for Plain and Reinforced Concrete. Bureau of Indian Standards: New Dehli, India, 2000.

37. Bao, X.; Demerchant, M.; Brown, A.; Bremner, T. Tensile and compressive strain measurement in the lab and field with the distributed Brillouin scattering sensor. *J. Light. Technol.* **2001**, *19*, 1698–1704.
38. Roux, S.; Hild, F. Stress intensity factor measurements from digital image correlation: Post-processing and integrated approaches. *Int. J. Fract.* **2006**, *140*, 141–157. [CrossRef]
39. Kim, B.; Weiss, W. Using acoustic emission to quantify damage in restrained fiber-reinforced cement mortars. *Cem. Concr. Res.* **2003**, *33*, 207–214. [CrossRef]
40. Hafezolghorani, M.; Farzad, H.; Ramin, V.; Jaafar, M.S.B.; Karimzade, K. Simplified damage plasticity model for concrete. *Struct. Eng. Int.* **2017**, *27*, 68–78. [CrossRef]
41. Yehia, S.; Abudayyeh, O.; Nabulsi, S.; Abdel-Qader, I. Detection of Common Defects in Concrete Bridge Decks Using Nondestructive Evaluation Techniques. *J. Bridge Eng.* **2007**, *12*, 215–225. [CrossRef]
42. Hognestad, E. *Study of Combined Bending and Axial Load in Reinforced Concrete Members*; Engineering Experiment Station, University of Illinois at Urbana Champaign, College of Engineering: Champaign, IL, USA, 1951.
43. Villain, G.; Sbartaï, Z.M.; Dérobert, X.; Garnier, V.; Balayssac, J.P. Durability diagnosis of a concrete structure in a tidal zone by combining NDT methods: Laboratory tests and case study. *Constr. Build. Mater.* **2012**, *37*, 893–903. [CrossRef]
44. Bogas, J.; Gomes, M.; Gomes, A. Compressive strength evaluation of structural lightweight concrete by non-destructive ultrasonic pulse velocity method. *Ultrasonics* **2013**, *53*, 962–972. [CrossRef] [PubMed]
45. Tran, Q.; Han, D.; Kang, C.; Haldar, A.; Huh, J. Effects of Ambient Temperature and relative humidity on subsurface defect detection in concrete structures by active thermal imaging. *Sensors* **2017**, *17*, 1718. [CrossRef] [PubMed]
46. Murad, Y.; Tarawneh, A.; Arar, F.; Al-Zu'bi, A.; Al-Ghwairi, A.; Al-Jaafreh, A.; Tarawneh, M. Flexural strength prediction for concrete beams reinforced with FRP bars using gene expression programming. *Structures* **2021**, *33*, 3163–3172. [CrossRef]
47. Xie, D.; Brantley, W.; Culbertson, B.; Wang, G. Mechanical properties and microstructures of glass-ionomer cements. *Dent. Mater. Off. Publ. Acad. Dent. Mater.* **2000**, *162*, 129–138. [CrossRef] [PubMed]
48. Li, V.; Liang, E. Fracture processes in concrete and fiber reinforced cementitious composites. *J. Eng. Mech. -ASCE* **1986**, *112*, 566–586. [CrossRef]
49. Abdel-Wahab, A.; Maligno, A.; Silberschmidt, V. Micro-scale modelling of bovine critical bone fracture: Analysis of crack propagation and microstructure using X-FEM. *Comput. Mater. Sci.* **2012**, *52*, 128–135. [CrossRef]
50. Devi, K.; Saini, B.; Aggarwal, P. Micro-structural analysis of cement composites using stone waste: A review. *IOP Conf. Ser. Mater. Sci. Eng.* **2022**, *1260*, 012031. [CrossRef]
51. Landis, E.; Keane, D. X-ray microtomography. *Mater. Charact.* **2010**, *61*, 1305–1316. [CrossRef]
52. Kotula, P.; Rohrer, G.; Marsh, M. Focused ion beam and scanning electron microscopy for 3D materials characterization. *MRS Bull.* **2014**, *39*, 361–365. [CrossRef]
53. Lange, D.; Jennings, H.; Shah, S. Relationship between fracture surface roughness and fracture behavior of cement paste and mortar. *J. Am. Ceram. Soc.* **1993**, *76*, 589–597. [CrossRef]
54. Launey, M.; Ritchie, R. On the fracture toughness of advanced materials. *Adv. Mater.* **2009**, *21*, 2103–2110. [CrossRef]
55. Miramini, S.; Sofi, M.; Aseem, A.; Baluwala, A.; Zhang, L.; Mendis, P.; Duffield, C. Health assessment of a pedestrian bridge deck using ground penetrating radar. *Electron. J. Struct. Eng.* **2018**, *18*, 30–37. [CrossRef]
56. Tchalla, A.; Belouettar, S.; Makradi, A.; Zahrouni, H. An ABAQUS toolbox for multiscale finite element computation. *Composites Part B Eng.* **2013**, *52*, 323–333. [CrossRef]
57. Lee, J.; Fenves, G.L. Plastic-damage model for cyclic loading of concrete structures. *J. Eng. Mech.* **2018**, *124*, 892–900. [CrossRef]
58. Lubliner, J.; Oliver, J.; Oller, S.; Onate, E. A plastic-damage model. *Int. J. Solids Struct.* **1989**, *25*, 299–326. [CrossRef]
59. Jin, C.Y.; Li, Y.Q.; Zhu, J.C.; Li, Y. A finite element analysis on compressive properties of ECC with PVA fibers. *IOP Conf. Ser. Mater. Sci. Eng.* **2019**, *544*, 11–16. [CrossRef]
60. Sikadur®-31 IN 2-Part Thixotropic Structural Epoxy Adhesive. Available online: https://ind.sika.com/en/construction/concrete-repair/bonding-primers/sikadur-31-in.html (accessed on 3 February 2024).
61. George, J.; Rama, J.K.; Kumar, M.S.; Vasan, A. Behavior of plain concrete beam subjected to three point bending using concrete damaged plasticity (CDP) model. *Mater. Today Proc.* **2017**, *4*, 9742–9746. [CrossRef]
62. Hashim, D.T.; Hejazi, F.; Lei, V.Y. Simplified constitutive and damage plasticity models for UHPFRC with different types of fiber. *Int. J. Concr. Struct. Mater.* **2020**, *14*, 45. [CrossRef]
63. An, D.; Zhang, Y.X.; Richard, C.Y. Numerical modelling of 3D concrete printing: Material models, boundary conditions and failure identification. *Eng. Struct.* **2024**, *299*, 104–117. [CrossRef]

Disclaimer/Publisher's Note: The statements, opinions and data contained in all publications are solely those of the individual author(s) and contributor(s) and not of MDPI and/or the editor(s). MDPI and/or the editor(s) disclaim responsibility for any injury to people or property resulting from any ideas, methods, instructions or products referred to in the content.